The low-temperature crystal structure of the multiferroic melilite Ca2CoSi2O7

Andrew Sazonov, Vladimir Hutanu, Martin Meven, Georg Roth, István Kézsmárki, Hiroshi Murakawa, Yoshinori Tokura, Bálint Náfrádi

Angaben zur Veröffentlichung / Publication details:

Sazonov, Andrew, Vladimir Hutanu, Martin Meven, Georg Roth, István Kézsmárki, Hiroshi Murakawa, Yoshinori Tokura, and Bálint Náfrádi. 2016. "The low-temperature crystal structure of the multiferroic melilite Ca2CoSi2O7." *Acta Crystallographica Section B: Structural Science, Crystal Engineering and Materials* 72 (1): 126–32. https://doi.org/10.1107/s2052520615023057.

Acta Cryst B
STRUCTURAL SCIENCE
CRYSTAL ENGINEERING
MATERIALS

ISSN 2052-5206

The low-temperature crystal structure of the multiferroic melilite $Ca_2CoSi_2O_7$

Andrew Sazonov,[a,b]* Vladimir Hutanu,[a,b] Martin Meven,[a,b] Georg Roth,[a] István Kézsmárki,[c] Hiroshi Murakawa,[d] Yoshinori Tokura[d,e,f] and Bálint Náfrádi[g]

[a]Institute of Crystallography, RWTH Aachen University, Aachen, Germany, [b]Jülich Centre for Neutron Science (JCNS) at Heinz Maier-Leibnitz Zentrum (MLZ), Garching, Germany, [c]Department of Physics, Budapest University of Technology and MTA-BME Lendület Magneto-optical Spectroscopy Research Group, Budapest, Hungary, [d]Multiferroics Project, ERATO, Japan Science and Technology Agency (JST), University of Tokyo, Tokyo, Japan, [e]Department of Applied Physics and Quantum Phase Electronics Center (QPEC), University of Tokyo, Tokyo, Japan, [f]Cross-Correlated Materials Research Group (CMRG) and Correlated Electron Research Group (CERG), RIKEN Advanced Science Institute, Wako, Japan, and [g]École Polytechnique Fédérale de Lausanne, Laboratory of Nanostructures and Novel Electronic Materials, Lausanne, Switzerland. *Correspondence e-mail: mail@sazonov.org

Received 15 July 2015
Accepted 1 December 2015

Edited by N. B. Bolotina, Russian Academy of Sciences, Russia

Keywords: magnetoelectric coupling; multiferroic melilite; twinning; single-crystal neutron diffraction.

CCDC reference: 1439868

Supporting information: this article has supporting information at journals.iucr.org/b

In the antiferromagnetic ground state, below $T_N \simeq 5.7$ K, $Ca_2CoSi_2O_7$ exhibits strong magnetoelectric coupling. For a symmetry-consistent theoretical description of this multiferroic phase, precise knowledge of its crystal structure is a prerequisite. Here we report the results of single-crystal neutron diffraction on $Ca_2CoSi_2O_7$ at temperatures between 10 and 250 K. The low-temperature structure at 10 K was refined assuming twinning in the orthorhombic space group $P2_12_12$ with a $3 \times 3 \times 1$ supercell [a = 23.52 (1), b = 23.52 (1), c = 5.030 (3) Å] compared with the high-temperature normal state [tetragonal space group $P\bar{4}2_1m$, $a = b \simeq 7.86$, $c \simeq 5.03$ Å]. The precise structural parameters of $Ca_2CoSi_2O_7$ at 10 K are presented and compared with the literature X-ray diffraction results at 130 and 170 K (low-temperature commensurate phase), as well as at $\sim$ 500 K (high-temperature normal phase).

1. Introduction

Recently, several members of the melilite family, such as $Ca_2CoSi_2O_7$, $Sr_2CoSi_2O_7$, $Ba_2MnGe_2O_7$ and $Ba_2CoGe_2O_7$, have been found to be multiferroic (see *e.g.* Murakawa *et al.*, 2012, and references therein). These materials show significant magnetoelectric coupling in many of their static and dynamic properties. For instance, in the recent work of Kézsmárki *et al.* (2014), it was shown *via* polarized terahertz spectroscopy studies on multiferroic $Ca_2CoSi_2O_7$, $Sr_2CoSi_2O_7$ and $Ba_2CoGe_2O_7$ that their magnetoelectric spin excitations exhibit quadrochroism: They have different colours for all four combinations of two propagation directions (forward or backward) and two orthogonal polarizations of a light beam. It was also recently shown by Perez-Mato & Ribeiro (2011) that the main features of the magnetoelectric behaviour can be predicted by symmetry considerations without appealing to any specific atomic mechanism. Thus a precise structural model is often essential for theoretical works. However, for many melilite systems, the structural information is still unavailable.

Due to the lack of low-temperature structural details, a general non-centrosymmetric tetragonal structure of melilites A_2BTO_7 with space group $P\bar{4}2_1m$ is often used (see, *e.g.*, the works of Kézsmárki *et al.*, 2014; Akaki *et al.*, 2009; Szaller *et al.*, 2014, and references therein). The melilite-type structure is represented in Fig. 1. It consists of TO_4 pairs that form the T_2O_7 dimers. These are linked together by the BO_4 tetrahedra

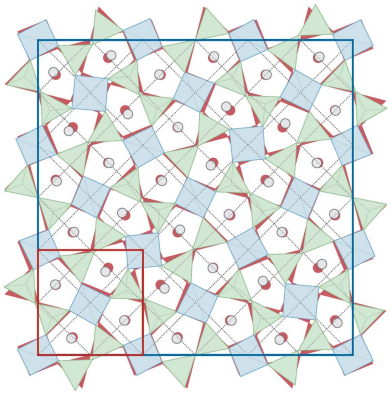

into layers stacked along the tetragonal [001] axis. The tetrahedral layers are connected by the large A cations. The above-mentioned simplifications are valid only at high temperatures where the tetragonal space group $P\bar{4}2_1m$ describes well the melilite crystal structure. At low temperatures, the crystal symmetry does not necessarily remain the same as in the high-temperature phase. An example is $Ba_2CoGe_2O_7$, where the orthorhombic polar space group $Cmm2$ was proposed as the true crystal structure (Hutanu *et al.*, 2011, 2012) to describe the multiferroic ground state.

In the case of $Ca_2CoSi_2O_7$, the temperature dependence of the structure is even more complex. Based on X-ray diffraction data between 30 and 600 K, $Ca_2CoSi_2O_7$ undergoes a series of structural phase transitions. The first corresponds to a normal to incommensurate (N–IC) transition and the second one is an incommensurate to commensurate (IC–C) transition. Accordingly, in the normal state above ~ 500 K the space group of $Ca_2CoSi_2O_7$ is $P\bar{4}2_1m$ (Fig. 1) with lattice parameters $a = b \simeq 7.86$ Å and $c \simeq 5.03$ Å (Kusaka *et al.*, 2001). X-ray diffraction and heat capacity measurements show that T_{N-IC} lies in the relatively narrow temperature range 478–498 K and does not depend on the thermal history of the sample (Hagiya *et al.*, 1993; Riester & Böhm, 1997; Kusaka *et al.*, 2001; Jia *et al.*, 2006). In the intermediate temperature range of 160–270 $\lesssim T \lesssim$ 480 K, an incommensurately modulated phase develops with two propagation vectors $\mathbf{k}_1 = q(\mathbf{a}^* + \mathbf{b}^*)$ and $\mathbf{k}_2 = q(-\mathbf{a}^* + \mathbf{b}^*)$, where q increases with a temperature decrease from ~ 0.29 up to 1/3 (Hagiya *et al.*, 2001). The published T_{IC-C} varies in the broad temperature range between 160 and 270 K (Riester & Böhm, 1997; Hagiya *et al.*, 2001; Jia *et al.*, 2006). Moreover, the IC–C transition is characterized by a prominent temperature hysteresis. Additionally, a significant difference of T_{IC-C} was found by X-ray or electron diffraction (Jia *et al.*, 2006). Below T_{IC-C}, a commensurately modulated lock-in structure appears with a $(3 \times 3 \times 1)$ supercell and lattice parameters $a \simeq b \simeq 23.51$ and $c \simeq 5.03$ Å (Riester *et al.*, 2000; Hagiya *et al.*, 2001). Two different structures with space groups $P\bar{4}$ and $P2_12_12$ were proposed to describe the crystal symmetry based on X-ray diffraction data. Riester *et al.* (2000) have assigned the space group $P\bar{4}$ to the structure based on the observed reflections violating the systematic extinction rule for $P2_12_12$. In the works of Hagiya *et al.* (2001) and Jia *et al.* (2006), those reflections were attributed to the multiple diffraction and the space group $P2_12_12$ was found to give better agreement for both pure and lightly Zn-doped $Ca_2CoSi_2O_7$. However, full diffraction data collection to refine the structural parameters was never performed below 130 K.

In order to fill this gap of low-temperature structural information on $Ca_2CoSi_2O_7$ and to provide reliable data for further experimental and theoretic research, we performed single-crystal neutron diffraction measurements at temperatures between 10 and 250 K. The results of the structure refinement at 10 K (just above $T_N \simeq 5.7$ K) are presented here and compared with X-ray diffraction data from literature collected in the low-temperature commensurate phase at 130 K in space group $P\bar{4}$ (Riester *et al.*, 2000) and 170 K in space group $P2_12_12$ (Hagiya *et al.*, 2001), as well as in the high-temperature normal phase at about 500 K in space group $P\bar{4}2_1m$ (Kusaka *et al.*, 2001).

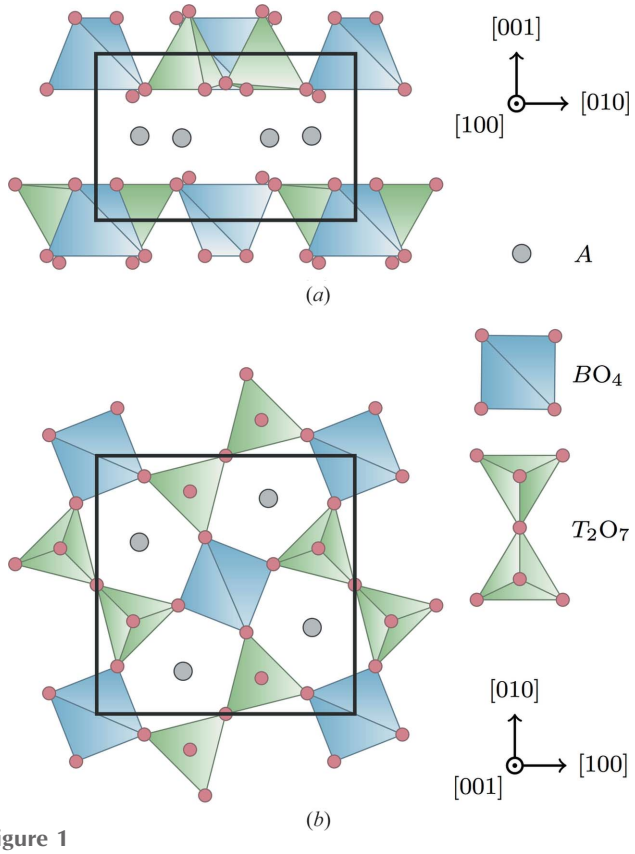

Figure 1
The average crystal structure of the melilite-type compounds of the general formula $A_2BT_2O_7$, which is described by a non-centrosymmetric tetragonal space group $P\bar{4}2_1m$.

2. Experimental

Single crystals of $Ca_2CoSi_2O_7$ were grown by the floating-zone technique and were characterized in previous studies (Kézsmárki *et al.*, 2014; Szaller *et al.*, 2014). The cylindrical sample used for neutron scattering experiments was approximately 4 mm high with about the same diameter.

Unpolarized single-crystal neutron diffraction studies were performed on the four-circle diffractometer HEiDi (Meven *et al.*, 2007) at the hot-neutron source of the FRM II reactor (Heinz Maier–Leibnitz Zentrum, Germany). A wavelength of $\lambda = 1.169$ Å was obtained from a Ge (311) monochromator with a high flux density of $\sim 1.2 \times 10^7$ neutrons s^{-1} cm^{-1} with an Er-filter to suppress the $\lambda/3$ contamination. For low-temperature experiments, a closed-cycle He cryostat was mounted in the Eulerian cradle of the diffractometer. The sample was wrapped in Al foil in order to ensure temperature homogeneity. The temperature was measured and controlled by a diode sensor near the heater position. The sample temperature was independently monitored by a second thermometer placed close to the sample position. A temperature stability of ± 0.1 K was achieved by this method. The

Table 1
Experimental details.

Crystal data	
Chemical formula	$Ca_2CoSi_2O_7$
M_r	307.26
Crystal system, space group	Orthorhombic, $P2_12_12$
Temperature (K)	10
a, b, c (Å)	23.52 (1), 23.52 (1), 5.03 (1)
V (Å^3)	2782.5
Z	18
D_x (Mg m^{-3})	3.304
Radiation type	Neutron, λ = 1.1695 Å
μ (mm^{-1})	0.02
Crystal form, colour	Cylinder, blue
Crystal size (mm)	4 × 2 (radius)
Data collection	
Diffractometer	Four-circle
Radiation source	Nuclear reactor
Monochromator	Ge (311)
Data collection method	ω scans
θ_{max} (°)	64.92
Absorption correction	–
$(\sin\theta/\lambda)_{max}$ (Å^{-1})	0.77
Range of h, k, l	$h = -20 \rightarrow 36$, $k = -30 \rightarrow 36$, $l = -7 \rightarrow 7$

temperature dependence of selected reflections were measured in the range of 10–250 K during cooling procedure. Full data collection was done at 10 K.

The corrected integrated intensities of the measured reflections were obtained with the *DAVINCI* program (Sazonov, 2015) using the Lehmann–Larsen method for peak location (Lehmann & Larsen, 1974). The structural parameters of $Ca_2CoSi_2O_7$ were refined using the *JANA*2006 program (Petříček *et al.*, 2014). Experimental details are summarized in Table 1.

3. Results and discussion

3.1. Low-temperature crystal structure model

Group-theoretical calculations show (McConnell, 1999) that only two subgroups of the high-temperature tetragonal space group $P\bar{4}2_1m$ (No. 113 according to Hahn, 1995) can describe the low-temperature modulation of the melilite structure. These are the tetragonal space group $P\bar{4}$ (No. 81) and the orthorhombic space group $P2_12_12$ (No. 18). Based on X-ray diffraction experiments, arguments for both space groups were put forward. Riester *et al.* (2000) used the space group $P\bar{4}$ to describe the stucture at 130 K, while Hagiya *et al.* (2001) performed refinement at 170 K in the space group $P2_12_12$. The choice of space group $P\bar{4}$ was based on the observation of the (h00) and (0k0) types reflections with h and $k = 2n + 1$, which are forbidden in $P2_12_12$.

A few extremely weak reflections of the same type were also present in our neutron data. A detailed analysis of both the measured peak profiles and integrated intensities favours the multiple diffraction origin of those reflections. Most of the collected scans look like statistical noise even for those reflections which are calculated to be the strongest in $P\bar{4}$. Moreover, the measured intensities of visible reflections are much smaller than expected ones. For instance, the calculated intensities of (21,0,0) and (23,0,0) reflections are similar and they are the strongest of this type. However, the measured intensity of (21,0,0) is about 20 times smaller compared with the calculations and (23,0,0) is not visible at all. This could be well explained by multiple diffraction, but not by the symmetry lowering. The same assumption was made in the work of Hagiya *et al.* (2001) based on the measurements of $Ca_2CoSi_2O_7$ at different diffraction conditions. In the lightly Zn-doped $Ca_2CoSi_2O_7$ no violation of the extinction rules for the space group $P2_12_12$ was observed by Jia *et al.* (2006). Finally, by means of neutrons with both short and long wavelengths we have clearly shown that the scattered intensities detected at the positions of forbidden reflections in the related melilite compound $Ba_2CoGe_2O_7$ are entirely due to the multiple diffraction (Sazonov *et al.*, 2015). Similar multiple diffraction effects were also found on bismuth metal oxides in other neutron diffraction studies (Birkenstock *et al.*, 2013). Thus we conclude that the above-mentioned reflections in $Ca_2CoSi_2O_7$ are caused by multiple diffraction. This is strong evidence against space group $P\bar{4}$ in favour of $P2_12_12$, because

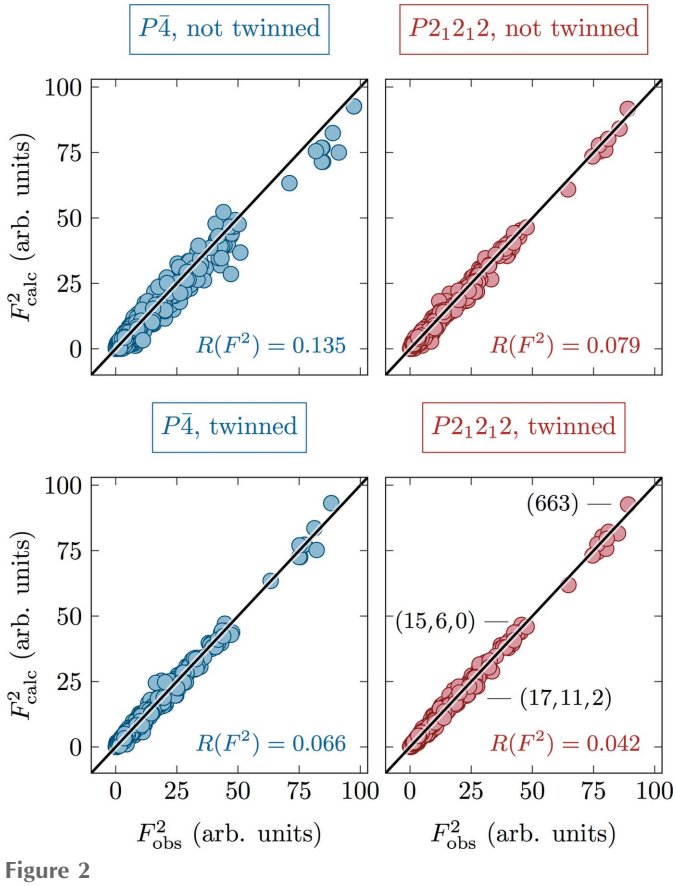

Figure 2
The quality of the $Ca_2CoSi_2O_7$ crystal structure refinement in different models: space groups $P\bar{4}$ (left column, blue circles) and $P2_12_12$ (right panel, red circles). The upper and lower rows indicate the results of the refinement without and with twinning, respectively. The experimentally measured and corrected integrated intensities (F^2_{obs}) are plotted against the calculated ones (F^2_{calc}). The intensities of a few selected Bragg reflections are marked.

Table 2
Single-crystal neutron diffraction experimental and refinement details in different models: space groups $P\bar{4}$ and $P2_12_12$ with and without twinning.

Model	$P\bar{4}$, not twinned	$P2_12_12$, not twinned	$P\bar{4}$, twinned	$P2_12_12$, twinned
Data collection				
No. of measured reflections	3127	3127	3127	3127
No. of independent reflections	2030	2006	2030	2006
No. of independent reflections with $I>3\sigma(I)$	1902	1883	1902	1883
R_{int}	0.020	0.018	0.020	0.018
Refinement				
Refinement on	F^2	F^2	F^2	F^2
$R[F^2>3\sigma(F^2)]$, $wR(F^2)$, S	0.135, 0.311, 9.92	0.079, 0.198, 6.34	0.066, 0.163, 5.22	0.042, 0.098, 3.17
No. of reflections	1902	1883	1902	1883
No. of parameters	166	167	167	168
Weighting scheme, w	$1/[\sigma^2(F_o^2)+0.0004F_o^4]$	$1/[\sigma^2(F_o^2)+0.0004F_o^4]$	$1/[\sigma^2(F_o^2)+0.0004F_o^4]$	$1/[\sigma^2(F_o^2)+0.0004F_o^4]$
Extinction correction	Isotropic, Gaussian Type 1†	Isotropic, Gaussian Type 1†	Isotropic, Gaussian Type 1†	Isotropic, Gaussian Type 1†
Extinction coefficient	0.036 (11)	0.037 (6)	0.023 (5)	0.036 (3)
Twin fraction	–	–	0.49 (1)	0.52 (1)

† According to Becker & Coppens (1974).

the calculated intensities are not reproduced in the experiment.

Nevertheless, both models were used in the refinement proses in order to determine the low-temperature crystal structure of $Ca_2CoSi_2O_7$ based on our neutron diffraction data at 10 K. The starting structural parameters were taken from the published structures determined by X-ray diffraction. In both cases, all atomic positions which are not fixed by symmetry were refined together with the isotropic atomic displacement (U_{iso}), scale and extinction parameters. The possibility that the low-temperature structure consists of two individuals of the same space-group symmetry which are twinned with respect to a diagonal mirror plane m_{xy} (Riester *et al.*, 2000; Hagiya *et al.*, 2001) was also taken into account. Thus, an additional refinement was performed with a twin fraction as the fitted parameter. The twin fraction represents the fractional volume of the crystal that the second domain occupies. In order to reduce the large number of fitted parameters, caused by the low-temperature tripling of the unit cell, atoms of the same type were constrained to have identical U_{iso} values. Besides this, no other constraints were used in the refinement process.

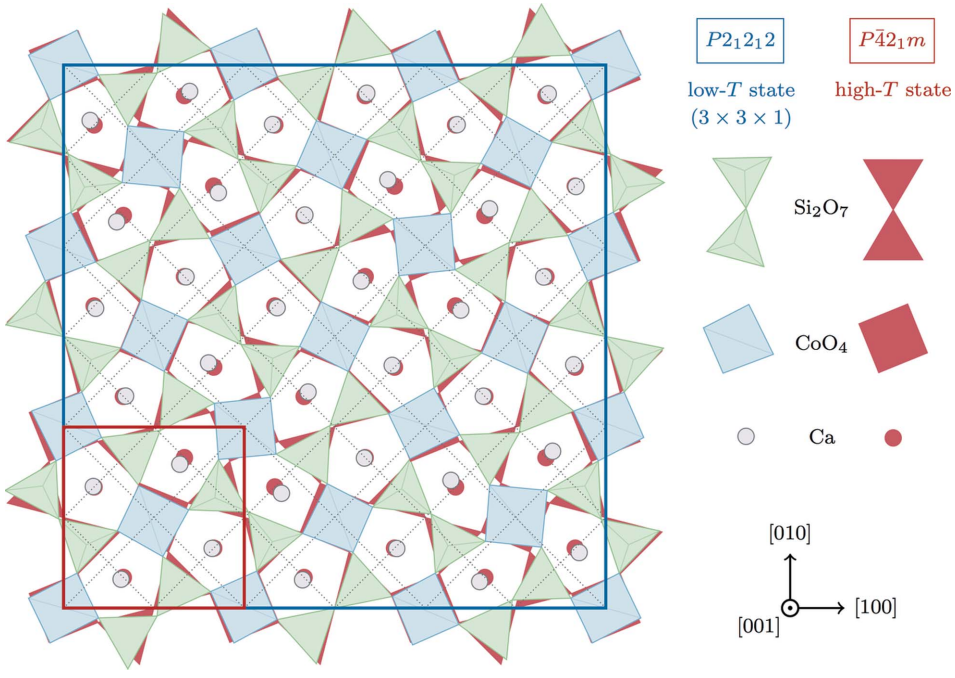

Figure 3
Comparison of the low-temperature commensurately modulated lock-in state (space group $P2_12_12$) with the high-temperature normal phase (space group $P\bar{4}2_1m$), according to our neutron diffraction data at 10 K and X-ray diffraction at ∼ 500 K (Kusaka *et al.*, 2001), respectively. The red square corresponds to $P\bar{4}2_1m$ and the blue one to the (3 × 3 × 1) supercell of $P2_12_12$.

Table 2 presents the resulted refinement parameters obtained in both $P\bar{4}$ and $P2_12_12$ space groups with and without twinning. The agreement between the experimental and calculated data is shown in Fig. 2. The introduction of twins significantly improves the quality of the fit for both cases. The twin fraction was found to be very close to a perfect twin value of 0.5.

Both models have a very similar number of parameters, which ensures well comparable statistical boundary conditions for the refinements. The ratio between the number of statistically significant independent reflections and the number of free parameters is more than 11, which support the sufficiency of the data basis. The reliability factors of the refinement for the $P2_12_12$ space group model are noticeably smaller then those for $P\bar{4}$. On average, they are increased by more than 60% in $P\bar{4}$ compared with $P2_12_12$.

Table 3
Fractional atomic coordinates (*x, y, z*) and isotropic atomic displacement parameters U_{iso} (Å^2) for the commensurately modulated lock-in phase of the ($3 \times 3 \times 1$) supercell refined in space group $P2_12_12$ (twinned with respect to m_{xy}) according to the present single-crystal neutron diffraction data at 10 K.

Atom	*x*	*y*	*z*	U_{iso}
Ca1	0.1086 (4)	0.0527 (4)	0.503 (3)	0.0075 (3)
Ca2	0.1145 (4)	0.3923 (4)	0.490 (2)	0.0075 (3)
Ca3	0.0554 (4)	0.2245 (5)	0.499 (3)	0.0075 (3)
Ca4	0.2746 (5)	0.1114 (4)	0.515 (2)	0.0075 (3)
Ca5	0.2677 (4)	0.4511 (4)	0.475 (2)	0.0075 (3)
Ca6	0.2153 (4)	0.2664 (3)	0.519 (2)	0.0075 (3)
Ca7	0.4409 (4)	0.0525 (4)	0.517 (2)	0.0075 (3)
Ca8	0.4505 (4)	0.3973 (4)	0.516 (2)	0.0075 (3)
Ca9	0.4028 (3)	0.2115 (4)	0.492 (2)	0.0075 (3)
Co1	0	0	0.014 (5)	0.0033 (7)
Co2	0.0057 (7)	0.3369 (7)	0.017 (3)	0.0033 (7)
Co3	0.1634 (9)	0.1612 (6)	0.001 (5)	0.0033 (7)
Co4	0.3347 (7)	0.0019 (8)	0.022 (3)	0.0033 (7)
Co5	0.3332 (9)	0.3299 (8)	0.009 (5)	0.0033 (7)
Si1	0.0418 (5)	0.1214 (5)	−0.066 (3)	0.0056 (3)
Si2	0.0506 (5)	0.4568 (4)	−0.080 (2)	0.0056 (3)
Si3	0.1241 (5)	0.2862 (4)	0.081 (2)	0.0056 (3)
Si4	0.2124 (5)	0.0411 (5)	0.071 (3)	0.0056 (3)
Si5	0.2160 (4)	0.3812 (5)	0.032 (2)	0.0056 (3)
Si6	0.2827 (4)	0.2081 (4)	−0.037 (2)	0.0056 (3)
Si7	0.3827 (5)	0.1234 (5)	−0.056 (3)	0.0056 (3)
Si8	0.3830 (4)	0.4549 (5)	−0.065 (3)	0.0056 (3)
Si9	0.4520 (4)	0.2811 (5)	0.056 (3)	0.0056 (3)
O1	−0.0083 (3)	0.1647 (3)	0.822 (2)	0.0080 (2)
O2	0.1740 (3)	−0.0146 (3)	0.174 (2)	0.0080 (2)
O3	0.1797 (3)	0.3265 (3)	0.172 (2)	0.0080 (2)
O4	0.3401 (3)	0.1758 (3)	0.836 (2)	0.0080 (2)
O5	0.5	0	0.205 (2)	0.0080 (2)
O6	0.0423 (3)	0.1183 (3)	0.245 (2)	0.0080 (2)
O7	0.0505 (3)	0.4582 (3)	0.235 (2)	0.0080 (2)
O8	0.1247 (3)	0.2822 (3)	0.751 (2)	0.0080 (2)
O9	0.2165 (3)	0.0436 (3)	0.754 (2)	0.0080 (2)
O10	0.2080 (3)	0.3847 (3)	0.722 (2)	0.0080 (2)
O11	0.2776 (3)	0.2032 (3)	0.274 (2)	0.0080 (2)
O12	0.3863 (3)	0.1209 (3)	0.258 (2)	0.0080 (2)
O13	0.3862 (3)	0.4584 (3)	0.263 (2)	0.0080 (2)
O14	0.4624 (3)	0.2760 (3)	0.744 (2)	0.0080 (2)
O15	0.0250 (3)	0.0620 (3)	0.771 (2)	0.0080 (2)
O16	0.0986 (3)	0.1435 (3)	0.773 (2)	0.0080 (2)
O17	0.0342 (2)	0.3955 (3)	0.777 (2)	0.0080 (2)
O18	0.1039 (3)	0.4798 (3)	0.754 (2)	0.0080 (2)
O19	0.1388 (3)	0.2266 (3)	0.225 (2)	0.0080 (2)
O20	0.0711 (3)	0.3125 (3)	0.224 (2)	0.0080 (2)
O21	0.1826 (3)	0.0953 (3)	0.224 (2)	0.0080 (2)
O22	0.2713 (3)	0.0301 (3)	0.230 (2)	0.0080 (2)
O23	0.1864 (3)	0.4357 (3)	0.206 (2)	0.0080 (2)
O24	0.2779 (3)	0.3794 (3)	0.171 (2)	0.0080 (2)
O25	0.2870 (3)	0.2728 (3)	0.834 (2)	0.0080 (2)
O26	0.2301 (3)	0.1799 (3)	0.795 (2)	0.0080 (2)
O27	0.3562 (3)	0.0674 (3)	0.792 (2)	0.0080 (2)
O28	0.4403 (3)	0.1371 (3)	0.788 (2)	0.0080 (2)
O29	0.3809 (3)	0.3879 (3)	0.831 (2)	0.0080 (2)
O30	0.4350 (3)	0.4821 (3)	0.782 (2)	0.0080 (2)
O31	0.4841 (3)	0.2276 (3)	0.219 (2)	0.0080 (2)
O32	0.3918 (3)	0.2831 (3)	0.181 (2)	0.0080 (2)

Moreover, in the $P2_12_12$ model all U_{iso} parameters are positive in contrast to $P\bar{4}$, where the values of the Co displacement parameters are fitted to be negative and thus non-physical. A negative value of isotropic ADPs from single-crystal neutron diffraction is evidence of a poor model. The same effect was found by Jia *et al.* (2006) in the treatment of the X-ray data for lightly Zn-doped $Ca_2CoSi_2O_7$.

The other possible differences between space groups $P2_12_12$ and $P\bar{4}$ are hidden due to the similar values of the *a* and *b* lattice parameters in the orthorhombic model (equal within experimental precision) and the presence of equally populated 90° twin domains (according to the structure refinement).

We have selected the space group $P2_12_12$ with twining as the most appropriate model to describe the neutron diffraction data of $Ca_2CoSi_2O_7$ at 10 K. Our choice is based on the larger reliability factors in $P\bar{4}$, non-physical values of ADPs in $P\bar{4}$ and multiple diffraction origin of the forbidden in $P2_12_12$ reflections. The orthorhombic model agrees with X-ray diffraction on $Ca_2CoSi_2O_7$ at 170 K (Hagiya *et al.*, 2001) as well as with the $Ca_2CoSi_2O_7$ magnetoelectric tensor measurements (Akaki *et al.*, 2014). Table 3 presents the refined atomic coordinates as well as the U_{iso} parameters for the commensurate lock-in phase of the ($3 \times 3 \times 1$) supercell in space group $P2_12_12$, twinned with respect to m_{xy}. Full details of the refinement, including bond lengths and angles, are given in the CIF file in the supporting information.

3.2. Low-temperature *versus* high-temperature state

Fig. 3 shows a comparison of the low-temperature commensurate lock-in $3 \times 3 \times 1$ state (space group $P2_12_12$) with the high-temperature normal phase (space group $P\bar{4}2_1m$), according to our neutron diffraction data at 10 K and X-ray diffraction at $\sim$ 500 K (Kusaka *et al.*, 2001), respectively. The largest shift in the atomic positions is found for x_{O29} which corresponds to approximately 0.5 Å.

A comparison of the structure at 10 K and that derived within the same model (space group $P2_12_12$) from X-ray diffraction at 170 K (Hagiya *et al.*, 2001) gives a much smaller difference in the positional parameters with an average value of $\sim 1\sigma$. The largest shift in the atomic positions of 0.09 Å is found for z_{Co1}. However, the average shift is less than 0.014 Å. Thus, we did not find any significant structural changes from T_{IC-C} down to at least 10 K.

At 10 K, the Si—O distances range between 1.549 (13) and 1.674 (13) Å. The Co—O bond lengths vary from 1.890 (16) to 1.997 (19) Å. The distances between the Ca and O atoms are in the range 2.288 (13)–2.444 (13) Å. The detailed values of the bond lengths and angles can be found in the CIF file.

3.3. Incommensurate to commensurate transition

The T_{N-IC} of $Ca_2CoSi_2O_7$ is well above room temperature, but T_{IC-C} lies in the studied temperature interval 10–250 K. In agreement with X-ray diffraction our neutron data show a significant number of superstructure reflections, which corresponds to the tripling of the high-temperature unit cell. A variation of the normalized integrated intensities of the main (12,3,0) and superstructure (820) Bragg reflections measured during the cooling process is presented in Fig. 4. Both main and superstructure peaks show similar temperature behaviour. Their intensities are constant from 250 K down to about 210 K. Below 210 K, the intensities start to increase by further cooling indicating an onset of the IC–C phase transition. The intensities of both reflections become constant again below

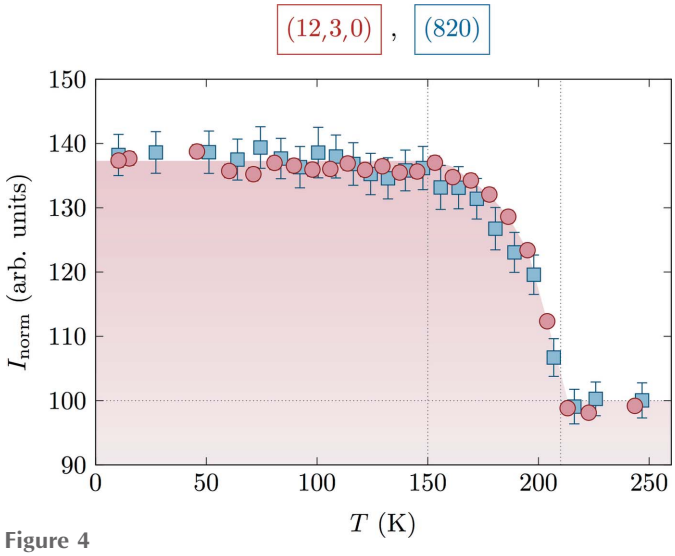

Figure 4
Temperature dependences of the normalized integrated intensities of the main (12,3,0) and superstructure (820) Bragg reflections shown in red circles and blue squares, respectively. The measurements were carried out during the cooling process.

~ 150 K. Their values are increased by approximately 40% compared with those at 210–250 K.

Fig. 5 shows a comparison of the main (15,12,2) and superstructure (17,11,2) Bragg reflection profiles at 10 K: Both have a similar intensity and full width at half maximum. The largest measured superstructure reflection is (17,11,2). Its intensity corresponds to ~ 20 % of the largest measured main (663) reflection.

4. Conclusions

Single-crystal neutron diffraction measurements on $Ca_2CoSi_2O_7$ were performed in the temperature range 10–250 K. A full data collection of more than 3000 Bragg reflections was performed at 10 K, close to the antiferromagnetic phase transition temperature $T_N \simeq 5.7$ K. The crystal structure was refined in the orthorhombic space group $P2_12_12$ with a tripled $(3 \times 3 \times 1)$ supercell, twinned with respect to m_{xy}. This model of the crystal structure was found to be preferable compared with the space group $P\bar{4}$. Our results agree with X-ray diffraction data treatment at 170 K as well as with the low-temperature magnetoelectric tensor measurements from the literature.

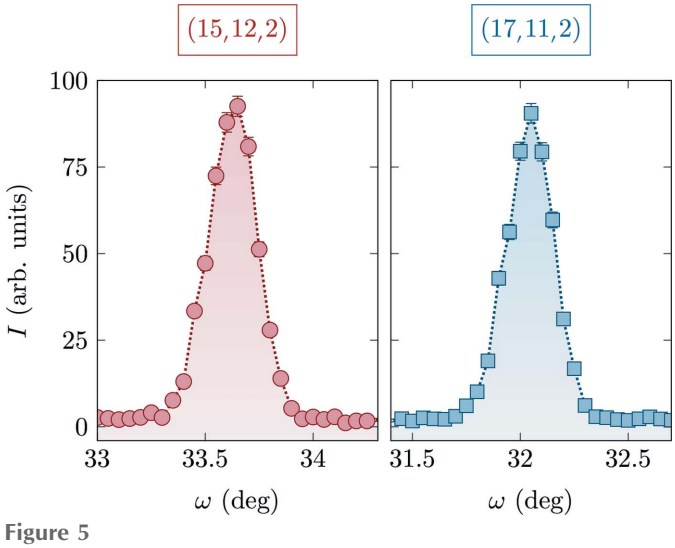

Figure 5
Comparison of the main (15,12,2) and superstructure (17,11,2) Bragg reflection profiles shown in the left (red circles) and right (blue squares) panels, respectively. The data were collected at 10 K.

Acknowledgements

This work is based upon experiments performed at the HEiDi instrument operated by RWTH Aachen/F2 Jülich (Jülich Aachen Research Alliance JARA) and was partly supported by BMBF under contract No. 05K13PA3. This project has also received funding from the European Union's Seventh Framework Program for research, technological development and demonstration under the NMI3-II Grant number 283883 and by the Hungarian Research Fund OTKA K108918. Work in Lausanne was supported by the Swiss National Science Foundation.

References

Akaki, M., Kuwahara, H., Matsuo, A., Kindo, K. & Tokunaga, M. (2014). *J. Phys. Soc. Jpn*, **83**, 093704.
Akaki, M., Tozawa, J., Akahoshi, D. & Kuwahara, H. (2009). *Appl. Phys. Lett.* **94**, 212904.
Becker, P. J. & Coppens, P. (1974). *Acta Cryst.* A**30**, 129–147.
Birkenstock, J., Nénert, G., Gesing, T. M., Burianek, M., Mühlberg, M. & Fischer, R. X. (2013). *Z. Kristallogr.* **228**, 611–619.
Hagiya, K., Kusaka, K., Ohmasa, M. & Iishi, K. (2001). *Acta Cryst.* B**57**, 271–277.
Hagiya, K., Ohmasa, M. & Iishi, K. (1993). *Acta Cryst.* B**49**, 172–179.
Hahn, T. (1995). Editor. *International Tables for Crystallography*, Vol. A. Dordrecht: Kluwer Academic Publishers.
Hutanu, V., Sazonov, A., Meven, M., Murakawa, H., Tokura, Y., Bordács, S., Kézsmárki, I. & Náfrádi, B. (2012). *Phys. Rev. B*, **86**, 104401.
Hutanu, V., Sazonov, A., Murakawa, H., Tokura, Y., Náfrádi, B. & Chernyshov, D. (2011). *Phys. Rev. B*, **84**, 212101.
Jia, Z. H., Schaper, A. K., Massa, W., Treutmann, W. & Rager, H. (2006). *Acta Cryst.* B**62**, 547–555.
Kézsmárki, I., Szaller, D., Bordács, S., Kocsis, V., Tokunaga, Y., Taguchi, Y., Murakawa, H., Tokura, Y., Engelkamp, H., Rõõm, T. & Nagel, U. (2014). *Nature Commun.* **5**, 1–9.
Kusaka, K., Hagiya, K., Okano, Y., Mukai, M., Iishi, K., Haga, N. & Ohmasa, M. (2001). *Phys. Chem. Miner.* **28**, 150–166.
Lehmann, M. S. & Larsen, F. K. (1974). *Acta Cryst.* A**30**, 580–584.
McConnell, J. D. C. (1999). *Z. Kristallogr.* **214**, 457–464.
Meven, M., Hutanu, V. & Heger, G. (2007). *Neutron News*, **18**, 19–21.
Murakawa, H., Onose, Y., Miyahara, S., Furukawa, N. & Tokura, Y. (2012). *Phys. Rev. B*, **85**, 174106.
Perez-Mato, J. M. & Ribeiro, J. L. (2011). *Acta Cryst.* A**67**, 264–268.
Petříček, V., Dušek, M. & Palatinus, L. (2014). *Z. Kristallogr.* **229**, 345–352.
Riester, M. & Böhm, H. (1997). *Z. Kristallogr.* **212**, 506–509.
Riester, M., Böhm, H. & Petricek, V. (2000). *Z. Kristallogr.* **215**, 102–109.
Sazonov, A. P. (2015). *Davinci*, http://sazonov.org/soft.html.

Sazonov, A., Meven, M., Roth, G., Georgii, R., Kezsmarki, I., Kocsis, V. & Hutanu, V. (2015). Arxiv:1511.02783.

Szaller, D., Bordács, S., Kocsis, V., Rõõm, T., Nagel, U. & Kézsmárki, I. (2014). *Phys. Rev. B*, **89**, 184419.